Lithographic engineering of anisotropies in (Ga,Mn)As

S. Hümpfner, K. Pappert, J. Wenisch, K. Brunner, C. Gould, G. Schmidt, and L.W. Molenkamp
Physikalisches Institut (EP3), Universität Würzburg, Am Hubland, D-97074 Würzburg, Germany

M. Sawicki and T. Dietl
Institute of Physics, Polish Academy of Sciences,
al. Lotników 32/46, PL-02668 Warszawa, Poland

(Dated: February 6, 2008)

The focus of studies on ferromagnetic semiconductors is moving from material issues to device functionalities based on novel phenomena often associated with the anisotropy properties of these materials. This is driving a need for a method to locally control the anisotropy in order to allow the elaboration of devices. Here we present a method which provides patterning induced anisotropy which not only can be applied locally, but also dominates over the intrinsic material anisotropy at all temperatures.

The coupling of transport and magnetic properties in ferromagnetic semiconductors gives rises to many interesting anisotropy related transport phenomena such as strong anisotropic magnetoresistance (AMR), in-plane hall [1], tunneling anisotropic magnetoresistance (TAMR) [2, 3] and Coulomb blockade AMR [4]. Studies on all of these effects so far have primarily made use of the intrinsic anisotropy present in the host (Ga,Mn)As layer. Before they can be harnessed to their full potential, a means of engineering the anisotropy locally is needed, such that multiple elements with different anisotropies can be integrated, and their interactions can be properly investigated.

One successful approach to local anisotropy control in metallic ferromagnets has been to make use of shape anisotropy. The same approach has been tried in the prototypical ferromagnetic semiconductor (Ga,Mn)As with lackluster results. In Ref. 5, the authors reported the observation of shape induced anisotropy in (Ga,Mn)As wires of 100 nm thickness x 1.5 x 200 μm^2, but only over a limited temperature range. Moreover, our own experience in attempting to use wires of similar dimensions have yielded sporadic results with the wires having irreproducible anisotropy, with either biaxial or uniaxial easy axes in inconsistent directions.

Furthermore, a simple calculation of the expected shape anisotropy term in such wires indicates that it should not play a significant role. While the infinite rod model used in [5] does predict an appreciable shape anisotropy field given by $\mu_0 M_S/2$, where M_S is the sample magnetization, it is not applicable to structures which are much thinner than their lateral dimensions. A more exact rectangular prism calculation [6] gives a 5 times weaker shape anisotropy with an anisotropy energy density of 80 J/m^3 which is much too small to compete with the typical crystalline anisotropy of 3000 J/m^3 [5, 7] in this material.

Growth strain reduces the cubic symmetry of the (Ga,Mn)As zinc-blend crystal structure creating a uniaxial anisotropy with an easy/hard magnetic axis in growth direction when the (Ga,Mn)As layer is tensile/compressively strained. This growth strain is known[8] to influence the strength of the perpendicular component of the anisotropy of the *whole* layer. Here we discuss (Ga,Mn)As grown on a (001) oriented GaAs substrate, whose out-of-plane hard magnetic axis confines the magnetization in the plane. Phenomenologically, the net in-plane magnetic anisotropy is known to result from a competition of two primary contributions: the crystal symmetry induced biaxial anisotropy with [100] and [010] easy axes, and a uniaxial anisotropy (the origin of which is not clear) with the direction of its easy axis assuming either of the in-plane $\langle 110 \rangle$ directions. The anisotropy of (Ga,Mn)As is further enriched by the existence of a second uniaxial, which is very weak and along [010] [2]. The interplay of these 3 anisotropies, all of which depend on hole concentration p, temperature T [9] and sample strain, leads to a material with a very sophisticated anisotropy which can be difficult to control or reproduce from one layer to the next.

In this letter we suggest that an additional agent, i.e., lithographically induced strain relaxation, also plays a significant role in nano-patterned structures and is the only reasonable means by which to properly exercise *local* control of the anisotropy in (Ga,Mn)As. We demonstrate that patterning imposed relaxation effects can not only be observed in ferromagnetic (Ga,Mn)As but also that these effects can dominate the magnetic anisotropy in the entire temperature range, up to the Curie temperature

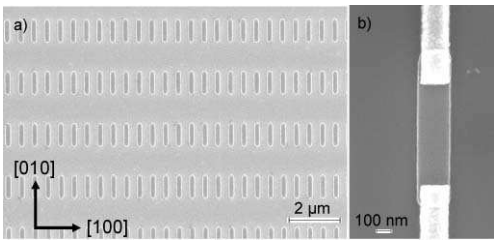

FIG. 1: **a**) SEM photograph of a small part of a typical 8 million nanobar array. The individual bars have lateral dimensions of 200 nm by 1 μm. **b**) An individual nanobar contacted for transport characterization.

T_c. Our findings pave the way to production of samples with *locally* designed anisotropy behavior.

A pair of nominally identical, high quality, 20 nm thick $Ga_{0.96}Mn_{0.04}As$ layers grown on a GaAs substrate [10] with a T_c of 70 K are chosen for these studies. They are patterned into arrays of either [100] or [010] oriented nanobars for magnetic investigation and equivalent individual nanobars contacted for transport investigations. Fig. 1 shows SEM photographs of the above mentioned structures. Each individual bar has lateral dimensions of 200 nm by 1 μm. The full array of them is defined using electron beam lithography with a negative resist. After developing, the defined pattern is transferred into the (Ga,Mn)As layer using chemically assisted ion beam etching (CAIBE). As many as 8 million nanobars are laid out to provide sufficient total magnetization for the magnetic anisotropy studies carried out in the variable temperature superconducting quantum interference device (SQUID) magnetometer.

We investigate the magnetization m vs. H dependencies of the sample in applied magnetic fields of up to $\pm$100 mT for the four major in-plane orientations. All spurious background signals originating from the substrate and sample holders are subtracted from the data presented.

The salient features of the SQUID investigations are summarized in Fig. 2, more elaborate magnetization studies of the magnetic anisotropy in such devices will be published elsewhere [11]. We start with the unpatterned, "parent" layer (top panels) to show that, as is typical for (Ga,Mn)As, it exhibits equivalent behavior along [100] and [010], both at very low T (Fig. 2(**a**)), and near T_C (Fig. 2(**b**)). This is simply a manifestation of the fact that the presence of a $\langle 110 \rangle$ uniaxial anisotropy, which bisects the four-fold $\langle 100 \rangle$ easy directions and acts equivalently on [100] and [010] does not break the symmetry between these directions. The [010] uniaxial anisotropy is too weak to measurably break the symmetry.

This behavior is in stark contrast to that of the patterned array, as shown in the bottom panels of Fig. 2, where magnetization studies of an array of nanobars oriented such that their long axis is along the [010] direction are presented. This axis is still a magnetic easy axis, similar to that of the host. The magnetic response along the [100] direction, which is along the short side of the nanobars has however been completely modified, and now exhibits pronounced hard axis behavior. From the hard axis measurements, we estimate the lithographically imposed anisotropy field $\mu_0 H_L$ produced by our sub-micron patterning to be 25 and 20 mT at 5 and 60 K, respectively. This field is comparable to the crystalline four-fold anisotropy field($\lesssim 100mT$) which dominates the behavior of the parent layer at 5 K, and is much larger than the $\langle 110 \rangle$ uniaxial term ($\sim 2mT$) which dominates the behaviour of the unpatterned layer at 60 K. For comparison, the shape anisotropy field is only 4 and 1.4 mT at these respective temperatures.

The overall magnetic anisotropy has thus been transformed from a strongly temperature dependent mixture of four-fold and uniaxial contributions into a well defined temperature independent uniaxial behavior imposed locally along the long axis of the nanobars. Arrays of nanobars patterned with their long axis along [100] give fully equivalent results.

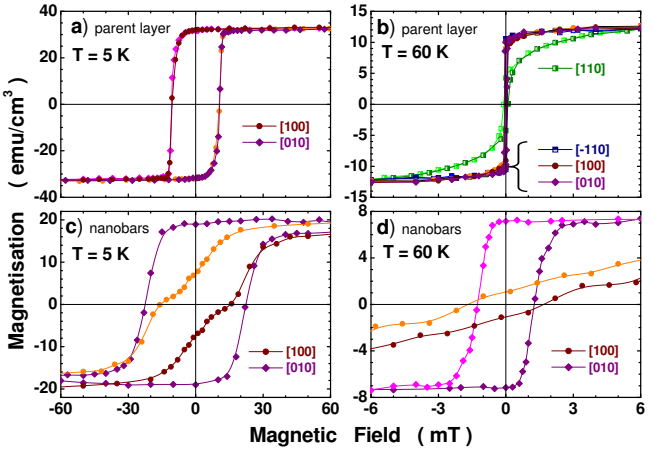

FIG. 2: (color online) SQUID magnetization data for (**a-b**) the parent layer and (**c-d**) the array of nanobars having their long side aligned to [010]. Light shades are used to mark the high resolution data obtained by numerical reflection to mimic the full hysteresis after confirming hysteretic symmetry with coarse measurements.

The submicron dimensions of the nanobars have also allowed us to reach the single domain limit in (Ga,Mn)As at low temperatures. As seen in Fig. 2c, the magnetization reversal along the easy axis of the nanobars takes place roughly at the uniaxial anisotropy field of 25 mT, indicating a nearly fully coherent behavior of the magnetization inside the nanobar. The situation is more complicated at 60 K where, despite a 20-fold increase in the coercivity of the nanobars compared to the parent layer, the easy axis switch occurs at $\sim$ 1.5 mT, which is only a small fraction of the lithographically imposed anisotropy field of 20 mT at that temperature. The reason for this is that the equivalence of the {[100], [010]} and $[\bar{1}10]$ anisotropy energy densities (Fig. 2b) observed in the parent layer at this temperature facilitates magnetization rotation along the nanobar, thus reducing their coercive field.

Having achieved the desired anisotropy control in the arrays, we now turn to electrical investigations, for which individual nanobars are prepared using similar lithography as in the patterning of the arrays. The major challenge in this case is a non-perturbative way of contacting the nanobar. This is non-trivial as it requires the formation of ohmic contacts onto (Ga,Mn)As with a $\sim$100 nm length scale. Moreover, our experience has shown that improperly optimized contacts do exert strain onto the layer, significantly altering it's anisotropy [12]. We succeeded by using a Ti layer patterned by lift-off as a mask. After etching, the Ti mask is removed, and Ti/Au con-

tacts are applied by e-beam lithography and lift-off. This yields contacts with a resistance-area product of below $10^{-6}\Omega \cdot cm^2$. In Fig. 3 we present transport characterization of two such nanobars patterned along the [100] and [010] directions on the same chip.

This sample is cooled in a variable temperature cryostat fitted with a vector field magnet, and its magnetoresistance (MR) behavior is measured for magnetic field applied along various angles φ (0° along [010]) in the plane of the layer. Prior to every scan, the sample is magnetized at -300 mT along φ.

The observed behavior (Fig. 3) is due to AMR, i.e. the fact, that the resistivity of a ferromagnetic material depends on the angle between the current and its magnetization. In (Ga,Mn)As the resistance is higher if the magnetization is perpendicular to the current($R_\perp$), than if both are parallel ($R_\parallel$). One can thus infer the angle ϑ between magnetization and current from the resistance R at any field value through[13]

$$R(\vartheta) = R_\perp - (R_\perp - R_\parallel)\cos^2\vartheta \qquad (1)$$

and from the magnetization behavior deduce the magnetic anisotropy of the (Ga,Mn)As stripes. The left part of Fig. 3 presents MR scans on the nanobar along the [010] crystal direction at various temperatures. A common feature is that field sweeps along the nanobar axis (0°, thick (red) line) yield a low resistance curve in the plot, indicating, through Eq. 1 that M remains parallel to the nanobar throughout the field sweep. The lowest resistance is observed also at zero external field, confirming that the nanobar axis is the magnetic easy axis in the whole temperature range. When the field is swept through positive values, the magnetization reversal process is seen at the same magnetic field values as in the magnetization measurements.

When the field is swept perpendicular to the nanobar (highest curves), the large values of the resistivity at high magnetic fields confirm that the magnetization is forced perpendicular to the nanobar. The resistance decreases monotonically as the field is swept down to zero where all curves meet, indicating that the magnetization always rotates to the same angle, i.e. to the uniaxial easy axis direction, previously established to be along the long axis of the nanobar. The linear slope seen to develop in the high magnetic field range is the isotropic magnetoresistance [14].

The right part of Fig. 3 presents results for the nanobar oriented along [100]. Since the coordinate system is fixed to the crystallographic axes, and not the axis of the nanobar, the fully opposite MR properties clearly indicate that the uniaxial behavior is related to the elongated shape of the nanobar. The parent layer easy axis perpendicular to the wire has been overwritten by the patterning process and the lithographically imposed uniaxial anisotropy is the dominant anisotropy up to T_c, as was seen in the magnetization investigations. Employing Eq. 1 allows us to assess the strength of this anisotropy. The

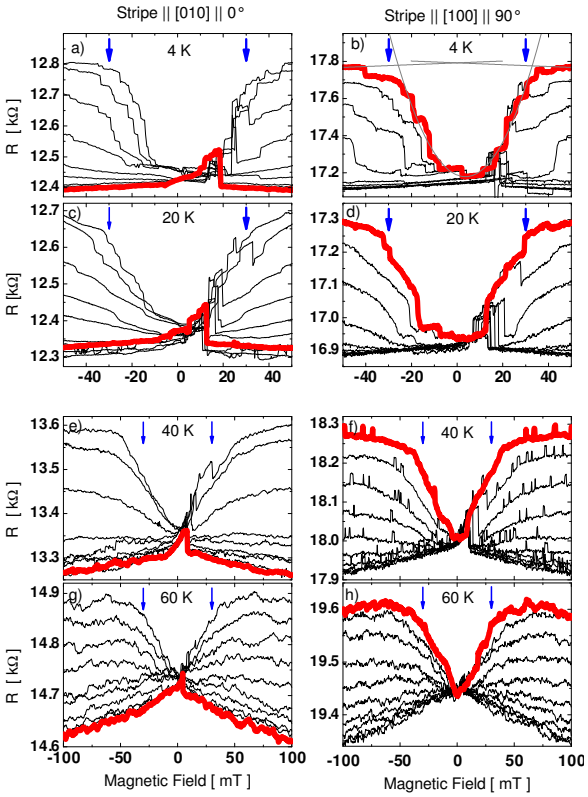

FIG. 3: Magnetoresistance scans for angles between 0° and 90° in 10° steps on the bars along [010] (left column) and [100] (right) at various temperatures and 5 mV bias voltage. The thick (red) line indicates the field sweep along the [010] crystal direction. The arrows indicate the estimated uniaxial anisotropy field.

hard axis MR-scan would be parabolic if only a pure uniaxial anisotropy was present. In such a case the magnetic field necessary to force the magnetization perpendicular to the easy axis is a direct measure for the strength of the anisotropy. To estimate this anisotropy field, we fit a parabola [15] to the low field data of the perpendicular field scan in Fig. 3b and interpolate the isotropic magnetoresistance of this scan back to the origin (thin grey lines). The fitted parabola is slightly shifted towards positive fields, which indicates the presence of a small biaxial anisotropy contribution. The intersections between the grey lines and the parabola give $\mu_0 H_L \sim 30$ mT. The same number (marked with blue arrows) is a reasonable estimate for $\mu_0 H_L$ in all parts of Fig. 3 indicating that indeed the lithography induced uniaxial anisotropy is almost unchanged between 4 K and 60 K. This is a strong indication that the present effect is fundamentally different from classic shape anisotropy, which depends on the volume magnetization, and thus decreases with increasing temperature until it vanishes at T_c. Moreover, while size effects may play a role in the observed increase of the coercive field, they would play no role in modifying the anisotropy. Obviously, the results presented here do not provide direct evidence of strain relaxation.

Direct confirmation would require x-ray diffraction measurement which are not possible on the small structures investigated here. However, we have been able to verify that strain relaxation is the important agent in the effects reported here using x-ray diffraction measurements on long and narrow etched (Ga,Mn)As stripes[16].

In conclusion, we have demonstrated a reliable technique for comprehensively controlling the anisotropy locally in (Ga,Mn)As using a lithographic technique. We believe this will prove itself a useful tool for studying novel spintronics effects related to transport between regions of different anisotropies or unique magnetization configurations within a layer.

Acknowledgments

The authors wish to thank V. Hock and T. Borzenko for help in sample fabrication, and to acknowledge financial support from the EU (NANOSPIN: FP6-IST-015728) and the German DFG (BR1960/2-2). Two of us (MS and TD) acknowledge JST (ERATO).

[1] H. X. Tang, R.K. Kawakami, D.D. Awschalom and M.L. Roukes *Phys. Rev. Lett.* **90**, 107201 (2003).
[2] C. Gould, C. Rüster, T. Jungwirth, E. Girgis, G.M. Schott, R. Giraud, K. Brunner, G. Schmidt, and L.W. Molenkamp *Phys. Rev. Lett.* **93**, 117203 (2004).
[3] C. Ruester et al., Phys. Rev. Lett. **94**, 027203 (2005)
[4] J. Wunderlich, T. Jungwirth, B. Kaestner, A. C. Irvine, A. B. Shick, N. Stone, K.-Y. Wang, U. Rana, A. D. Giddings, C. T. Foxon, R. P. Campion, D. A. Williams, and B. L. Gallagher, Phys. Rev. Lett., **97**, 077201 (2006).
[5] a) K. Hamaya, T. Taniyama, T. Koike and Y. Yamazaki, J. Appl. Phys. **99**, 123901 (2006) b) K. Hamaya, R. Moriya, A. Oiwa, T. Taniyama, Y. Kitamoto, and H. Munekata, IEEE Trans. Magn. **39**, 2785 (2003).
[6] A. Aharoni, J. Appl. Phys. **83**, 3432 (1998).
[7] K.Y Wang, M. Sawicki, K.W. Edmonds, R.P. Campion, S. Maat, C.T. Foxon, B.L. Gallagher, and T. Dietl, Phys. Rev Lett. **95**, 217204 (2005); and references therein.
[8] a)A. Shen, A. Oiwa, A. Endo, S. Katsumoto, Y. Iye, H. Ohno, F. Matsukura, Y. Sugawara, N. Akiba, and T. Kuroiwa, J. Cryst. Growth **175/176**, 1069 (1997) b)T. Dietl,H. Ohno and F. Matsukura, PRB **63**, 195205 (2001).
[9] M. Sawicki, K-Y. Wang, K.W. Edmonds, R.P. Campion, C.R. Staddon, N.R.S. Farley, C.T. Foxon, E. Papis, E. Kamiska, A. Piotrowska, T. Dietl, and B.L. Gallagher, Phys. Rev. B **71**, 121302(R) (2005).
[10] For details of the growth, see G.M. Schott, G. Schmidt, G. Karczewski, L.W. Molenkamp, R. Jakiela, A. Barcz, Appl. Phys. Lett., **82**, 4678 (2003)
[11] M. Sawicki et al., in preparation.
[12] C. Gould, K. Pappert, G. Schmidt, and L.W. Molenkamp, to be published in Adv. Mat.
[13] J. P. Jan, in "Solid State Physics" (Eds: F. Seitz, D. Turnbull), Academic Press Inc., New York, 1957.; T.R. McGuire, R.I. Potter, *IEEE Trans. Magn.* **MAG-11**, 1018 (1975).
[14] F. Matsukura, M. Sawicki, T. Dietl, D. Chiba, and H. Ohno, Physica E **21** (2004) 1032.
[15] F.G. West, Nature **188**, 129 (1960).
[16] J. Wenisch, L. Ebel, C. Gould, G. Schmidt, L.W. Molenkamp, and K.Brunner, MBE2006 Abstract Workbook, P.63 (2006)